Biology, Chemistry, and Environmental Sciences
Faculty Articles and Research

Biology, Chemistry, and Environmental Sciences

2013

Development of Self-Assembling Mixed Protein Micelles with Temperature-Modulated Avidities

Allyson S.C. Soon
Emory University

Michael H. Smith
Georgia Institute of Technology

Emily S. Herman
Georgia Institute of Technology

L. Andrew Lyon
Chapman University, lyon@chapman.edu

Thomas H. Barker
Emory University

Follow this and additional works at: http://digitalcommons.chapman.edu/sees_articles

Part of the Chemistry Commons

Recommended Citation

Development of Self-Assembling Mixed Protein Micelles with Temperature-Modulated Avidities

Development of Self-Assembling Mixed Protein Micelles with Temperature-Modulated Avidities

Allyson S.C. Soon[1,2], **Michael H. Smith**[2,3], **Emily S. Herman**[2,3], **L. Andrew Lyon**[2,3], and **Thomas H. Barker**[1,2,*]

[1]W. H. Coulter Department of Biomedical Engineering, Georgia Institute of Technology/Emory University, Atlanta, GA 30332, USA

[2]Petit Institute for Bioengineering and Bioscience, Georgia Institute of Technology, Atlanta, GA 30332, USA

[3]School of Chemistry and Biochemistry, Georgia Institute of Technology, Atlanta, GA 30332, USA

Abstract

Elastin-like polypeptides (ELPs) are polypentapeptides that undergo hydrophobic collapse and aggregation above a specific transition temperature, T_t. ELP diblocks sharing a common "core" block (I60) but varying "outer" blocks (A80, P40) were designed, where $T_{t,I} < T_{t,A} < T_{t,P}$. The formation of ~55 nm diameter mixed micelles from these ELP diblocks was verified using dynamic light scattering (DLS), multiangle light scattering (MALS) and fluorescence resonance energy transfer (FRET). To confer affinity to the blood circulating protein fibrinogen, a fibrinogen-binding tetrapeptide sequence (GPRP) was fused to A80-I60, while P40-I60 was fused to a non-binding control (GPSP). The self-assembling, peptide-displaying, mixed micelles exhibit temperature-modulated avidities for immobilized and soluble fibrinogen at 32 °C and 42 °C. In this initial proof-of-concept design, the engineered mixed micelles were shown to disengage fibrinogen at elevated temperatures. The modular nature of this system can be used for developing *in vivo* depot systems that will only be triggered to release *in situ* upon specific stimuli.

Keywords

affinity; elastin-like polypeptides; fibrinogen; self-assembly; temperature-responsive

1. Introduction

The array of switchable systems designed using stimuli-responsive materials has grown tremendously in recent years. In particular, polymers that undergo phase transitions in response to changes in temperature and pH have been employed in the creation of a variety of stimuli-responsive conjugates, interfaces and nanocarrier systems.[1-3] Given advances in protein synthesis and recombinant DNA technology, many of these stimuli-responsive systems can now be recapitulated using peptide-based biopolymers.[4, 5] Elastin-like polypeptides (ELPs) are chemically or recombinantly synthesized biopolymers modeled after repeating sequences in the mammalian elastin protein. Above a transition temperature, T_t, ELPs reversibly self-assemble by hydrophobic association, forming micron-sized aggregates that then coalesce to form a dense coacervate.[6] ELPs reported in literature

commonly comprise repeats of the pentapeptide sequence, VPG$\underline{X}$G, where the guest residue X is varied to create ELPs with different T_t.[7, 8]

The thermally-induced hydrophobic collapse and aggregation of ELPs has traditionally been utilized as a convenient means of purifying ELPs and ELP-fused proteins in a process known as inverse transition cycling.[9-11] Drawing from this concept, the fusion of two ELP blocks with different T_t can result in the formation of stable nanoscale micellar structures following the collapse of the block with the lower T_t.[12-14] Self-assembling triblock and multiblock ELPs have also been generated that capitalize on selective block collapse to form an initial network that can be stabilized through covalent crosslinks.[15, 16] The ability to produce high yields of ELPs with specific sequences has enabled the development of ELP nanostructures and materials with carefully tuned microscopic and macroscopic properties for diverse biomedical and biotechnological applications.[17]

A parallel area of ELP research capitalizes on the polymer chain conformation transition to effect a mechanical contraction. The potential for the use of ELPs as free energy transducers or molecular motors was first demonstrated by Urry et al. around the mid-1980s.[18] Given growing interests in this application, the mechanism behind the conformational transition of model ELP polypeptides has been studied by several different groups over the past decade.[19-22] Indeed, proteins containing short ELP sequences in place of their native linker sequences have been shown to exhibit temperature-modulated affinities for their respective ligands,[23, 24] setting the precedent for the rational design of stimuli-responsive biological switches using these contractile proteins.

This work brings together these lines of research by designing two ELP diblocks that should assemble to form a temperature-responsive peptide-displaying mixed micelle. These ELP diblocks share a common C-terminal "core" ELP block (I60) but varying N-terminal "outer" ELP blocks (A80, P40), where $T_{t,I} < T_{t,A} < T_{t,P}$. We hypothesized that the two diblocks (A80-I60, P40-I60) would form mixed micelles upon the collapse of I60, then exhibit sequential collapse of the outer block, A80, then P40 (**Figure 1).** This sequential collapse should allow the selective display and retraction of the outer end of the A80 block as the mixed micelles are brought above and below $T_{t,A}$, without triggering coacervation of the entire mixture due to the hydration shell afforded by P40.

As proof of principle, we expressed the fibrinogen-binding tetrapeptide GPRP (or the non-binding control tetrapeptide GPSP) sequence on the N-terminus of the A80-I60 diblock to study the interaction of the peptide-displaying mixed micelles with fibrinogen at different temperature regimes. The highly specific interaction of this tetrapeptide "knob" sequence with their corresponding "holes" on fibrinogen has been studied extensively by our group and others.[25-27] Therefore, we expect that the formulated self-assembling peptide-displaying mixed micelles will display GPRP and bind to fibrinogen at ambient conditions (below $T_{t,A}$), but not at physiological conditions (above $T_{t,A}$) due to selective outer block collapse.

2. Results and Discussion

2.1. ELP diblock recombinant protein production

The simplest ELPs are designed using aliphatic amino acids as guest residues since these uncharged non-polar residues primarily respond to temperature for the thermodynamically driven collapse of the hydrated protein chain.[28] Their transition temperatures typically fall within the experimentally accessible range from approximately 5 °C for poly(VPG$\underline{L}$G) to 55 °C for poly(VPG$\underline{G}$G).[7] Using recombinant protein design and production, Chilkoti's group has conducted extensive studies on the effects of ELP chain length, composition and

concentration on the thermal transitioning behavior of ELPs containing glycine, alanine, and/or valine as guest residues.[29, 30] Along these lines, we have chosen to work with the guest residues isoleucine (for the I60 block), alanine (for the A80 block), and proline (for the P40 block) in the design of our temperature-responsive peptide display system. As a point of interest, the presence of proline in the fourth position of the consensus VPGXG sequence is widely thought to interfere with the transitioning of the sequence.[7] This property is ideal in our system as a means of preserving the structural integrity of the self-assembled mixed micelles, even at elevated physiological temperatures.

The coding sequences for the ELP diblocks were successfully created and amplified using the pUC19 plasmid (details in Supplementary Information S1). These coding sequences were inserted into modified pET15b vectors, and then transformed into E. coli BL21(DE3) for IPTG (isopropyl β-D-1-thiogalactopyranoside)-induced protein expression. The myc-tagged proteins were purified from the bacterial host proteins via inverse transition cycling, cleaved with thrombin to expose the desired N-terminal peptide sequence, then re-purified via inverse transition cycling to remove the cleaved myc tag and thrombin. The following proteins were successfully produced: GPRP-A80-I60, GPSP-A80-I60, GPRP-P40-I60, GPSP-P40-I60. The same set of proteins containing an additional C-terminal cysteine for conjugation of the sulfhydryl functional group to maleimide-functionalized labels was also successfully generated.

2.2. Evaluating protein transition characteristics using SYPRO Orange

The SYPRO Orange thermal stability assay was used to evaluate the phase transition behavior of the ELP diblocks with temperature ramping. SYPRO Orange is an environment-sensitive dye used in high throughput thermal stability or protein aggregation assays.[31] Transition temperatures of ELP diblock solutions could be identified by a rapid increase in fluorescence output, corresponding to a peak in the first derivative (**Figure 2A,B**).

The results indicate the presence of two transitions for all the ELPs, including mixtures of different ELP diblocks. The close proximity of the first transition temperature, T_{t1}, for all the solutions at a given ELP concentration (**Figure 2C**) strongly suggests that this transition is associated with the collapse of the common core I60 block, or the self-assembly of ELP diblocks to form micelles. The second transition temperature, T_{t2}, identified was dependent on the identity and relative proportion of the variant outer ELP block, A80 or P40, in the protein solution (**Figure 2D**), suggesting that this temperature is associated with the transition of the outer shell. This may reflect micelle aggregation as the micelle shell collapsed, or overall destabilization of micellar structure to form growing ELP aggregates. This also implies that the SYPRO Orange assay is useful for identifying gross structural changes of proteins in solution, but is not applicable for monitoring subtle changes associated with specific ELP block collapse within a mixture of ELP blocks.

The intermediate T_{t2} identified for mixtures of GP(R/S)P-A80-I60 and GPSP-P40-I60, instead of three transition points corresponding to the transition for each block, is highly suggestive of the formation of mixed micelles comprising both species within a single assembly. In other words, the formation of distinct micelle populations of GP(R/S)P-A80-I60 and GPSP-P40-I60 should have resulted in three transition temperatures as the GP(R/S)P-A80-I60 micelles aggregated ahead of the GPSP-P40-I60 micelles as the temperature was ramped up. Since this was not observed, this suggests that the different ELP diblocks formed mixed assemblies upon the collapse of the common I60 block.

2.3. Micelle characterization using light scattering

To obtain the optimal protein concentration range for evaluation of micelle size, a dilution series of ELP diblock was generated and tested using DLS (see Supplementary Information S2). The amplitudes of the autocorrelation function were found to be comparable at 4 μM of protein and above, prompting our use of 10 μM solutions in subsequent assays.

The ELP diblocks form low dispersity (polydispersity < 15%) populations of ~55 nm in diameter (**Figure 3A**). This is consistent with previously reported data using ELP diblocks of comparable molecular weight and composition.[12] Notably, the hydrodynamic radius (R_h) of GP(R/S)P-A80-I60 is approximately 3 nm larger than that of GP(R/S)P-P40-I60, likely due to the slightly longer length of the GP(R/S)P-A80-I60 chain (comprising 140 pentapeptide repeats) compared to the GP(R/S)P-P40-I60 chain (100 repeats).

Results from the SYPRO Orange assay suggested a second transition point (T_{t2}) at about 40, 55 and 50 °C for 10 μM solutions of GP(R/S)P-A80-I60, GP(R/S)P-P40-I60, and GP(R/S)P-A80-I60 mixtures respectively. This approximates the temperatures at which the amplitude of the autocorrelation functions dropped drastically and appears to be associated with the formation of polydisperse micron-sized aggregates. Evaluation of the solutions using a cloud point measuring cell also suggests that T_{t2} is associated with the cloud point of the solutions (**Figure 3B**).

To evaluate the coordination number (Z) and elucidate the structure of the ELP micelles, MALS was performed. Despite differences in the Mw values between micelles, the particles showed similar root mean square radius (R_{rms}) values and coordination numbers (**Table 1**). The measure of R_h combined with R_{rms} enabled the calculation of the ρ ratio (R_{rms}/R_h). This ratio provides topological information since the R_{rms} is a size measurement, weighted by the mass distribution of polymer segments about the center of mass, whereas the R_h is inferred from the diffusion coefficient of the sphere. For spherical particles homogeneous in mass distribution, the ρ value is ~0.77. In contrast, the ρ ratio for the micelles investigated in this work (< 0.65) is suggestive of particle heterogeneous in density, with greater polymer mass located within the interior than the exterior of the structure. Similar values of ρ have been reported previously, where the lower value was attributed to inhomogeneous packing within the micelles.[12]

2.4. Micelle characterization using AFM

Micelle formation was further validated by atomic force microscopy (AFM) following dip coating of glass coverslips with ELP solutions above T_{t1}. The presence of roughly spherical nanoparticles with dimensions of the same order of magnitude as those from the light scattering data suggests that these are ELP micelles (**Figure 4A-C**). We further evaluated the heights of the features to obtain a measure of average particle size. The results suggest the formation of particles with an average particle height of 12.3 ± 2.3 nm for GPRP-A80-I60, 11.7 ± 3.9 nm for GPSP-P40-I60, and 17.6 ± 4.7 nm for a 1:4 mixture of the two ELPs. The comparatively larger particle widths observed (reading off from the x-axis of the height profiles in Figure 4) may be indicative of a flattening of the micelles during sample drying, which is also consistent with the smaller-than-expected particle heights compared to the MALS data (Table 1). To verify that the observed features are protein assemblies rather than mere artifacts from the sample preparation process, dip coating of glass coverslips conducted at ambient temperatures (~23 °C; below T_{t1}) yielded debris with height profiles around 2 nm, which is characteristic of the small, unstructured peptide aggregates expected at temperatures where micelles do not form.

2.5. Micelle characterization using FRET

The functionality of this self-assembling, peptide-displaying, micelle system relies on the formation of mixed micelles by ELP diblocks sharing a common core I60 block. FRET was used to demonstrate that mixed micelles comprising both ELP diblock species (particularly GPRP-A80-I60 and GPSP-P40-I60) were formed. Briefly, the C-terminal cysteine at the end of the I60 block of each ELP diblock species was conjugated to either the Alexa Fluor 488 or Alexa Fluor 546 via sulfhydryl-maleimide chemistry. These fluorophores should therefore localize within the core of the micelle resulting from the collapse of the I60 block. Given the Förster radius of 6.31 nm for this FRET pair and the R_{rms} of at least 15 nm for the micelles, we should observe a minimum FRET signal if the distinct ELP diblock species formed distinct micelle populations. Conversely, a strong FRET signal would suggest colocalization of the I60 block from distinct ELP diblock species within the same micelle core.

As expected, FRET, indicated by a reduction in AF488 emission ($I_{Em,d}$) and concomitant increase in AF546 emission ($I_{Em,a}$), was not observed in mixtures at ambient temperatures (**Figure 5A**), but was observed at temperatures above T_{t1} (~29 °C for a 1 μM protein solution; Figure 2C). The emission spectra of control wells containing either the respective AF488-labeled or AF546-labeled proteins did not change appreciably with temperature (data not shown). Quantifying this change as fold change of the acceptor emission divided by the fold change in donor emission (F_a/F_d), FRET increased from 25 °C to 35 °C, then stabilized at about 2.4 for all the mixtures tested (**Figure 5B**). Interestingly, F_a/F_d for the GPRP-A80-I60-AF488 with GPRP-A80-I60-AF546 positive control showed a slight upward trend above 40 °C, which may be suggestive of a reorganization of micellar core structure above T_{t2} of the protein solution (~40.5 °C for 1 μM GPRP-A80-I60; Figure 2D). Nonetheless, the close proximity of the results from all three mixtures suggests that both fluorophores were colocalized within the micelle core, regardless of the identity of the variant outer ELP block, A80 or P40.

We proceeded to evaluate the F_a/F_d ratios of mixtures of pre-formed micelles (**Figure 5C**). Solutions containing 1 μM of the indicated labeled ELP diblock were pre-incubated at 35 °C, where we expect micelle formation, then mixed at the pre-warmed plate reader before taking measurements (pre-cooling). Due to the micelle R_{rms} of at least 15 nm (Table 1), we should see minimum FRET as the respective fluorophores should be localized within their respective micelle cores. We then allowed these mixtures to cool down to room temperature (~22 °C) for an hour before re-heating to 35 °C to take a second reading (post-cooling). Due to the disassembly of micelles upon cooling, and their reassembly upon heating, we would expect to observe FRET at this point if the two species of ELP diblocks came together to form mixed micelles. As expected, the results suggest that the F_a/F_d ratio of mixtures of pre-formed micelles (pre-cooling) was significantly lower (* p < 0.001) than the F_a/F_d ratio post-cooling, where we expect the formation of mixed micelles. Moreover, the F_a/F_d ratios for these mixtures were not significantly different from corresponding premixed controls where solutions of the ELP diblocks were already mixed before the first incubation at 35 °C. This appears to further suggest that the assembly of these mixed micelles is spontaneous and reversible.

2.6. Binding specificity of ELP diblocks

The binding of fibrinogen to immobilized ELP diblocks was evaluated using a standard plate-based enzyme-linked immunosorbent assay (ELISA) format. As expected, the results indicate that fibrinogen bound specifically to GPRP-A80-I60-C and GPRP-P40-I60-C but not their respective GPSP-displaying controls (**Figure 6A**). This assay demonstrates the specificity of the GPRP:fibrinogen interaction, validates the use of the GPSP tetrapeptide

sequence as the non-binding control, and also indicates the absence of non-specific interactions between the ELP chains and fibrinogen. Interestingly, more fibrinogen bound to saturated GPRP-displaying ELP-coated wells than saturated GPRP-displaying peptide-coated wells (% normalized signal > 100), possibly indicative of steric hindrance when binding to GPRP presented in close proximity to the surfaces of the well. The binding specificity of the displayed GPRP, versus the control GPSP peptide at elevated temperatures was also verified (see Supplementary Information S3).

2.7. Binding specificity of mixed micelles

The binding of mixed micelles to immobilized fibrinogen was evaluated using a plate-based format similar to an ELISA. This assay was specifically designed to monitor the binding of mixed micelles, not just (possibly) monomeric ELP diblocks, to immobilized fibrinogen. Rather than label all the ELP diblocks, only the non-fibrinogen binding GPSP-P40-I60 was labeled with AF546. This labeled protein was mixed with the unlabeled "functional component" of the mixed micelle that would be expected to bind to fibrinogen (i.e. GPRP-A80-I60 or GPRP-P40-I60). Any GPSP-P40-I60-AF546 associated with the immobilized fibrinogen is interpreted as having been retained in the wells as part of a mixed micelle with the unlabeled functional component.

As expected, no significant fluorescence was observed at 22 °C, where the ELP diblocks were expected to exist as monomers (**Figure 6B**). At 32 °C, where micelle formation was verified, fluorescence was observed in the presence of GPRP-A80-I60 and GPRP-P40-I60 but not the GPSP controls. This indicates that the unlabeled functional component was successful in retaining the labeled non-fibrinogen-binding GPSP-P40-I60-AF546 within the wells, likely as part of a mixed micelle.

2.8. Interaction of mixed micelles with soluble fibrinogen using turbidity

As both the GPRP-displaying micelles and hole-containing fibrinogen are multivalent entities, we expect to see network formation and an increase in mixture turbidity as these components interact with each other. The extinction at $\lambda = 350$ nm has traditionally been used as a measure of fibrin fibril assembly as described in Weisel and Nagaswami.[32] We have also shown in an earlier publication that the addition of equimolar amounts of multivalent GPRP-displaying polyethylene glycol conjugates to fibrinogen increases solution turbidity at $\lambda = 350$ nm.[33] Changes in mixture turbidities at the different temperature regimes would thus be suggestive of variable micelle avidities (hence variable micelle-fibrinogen interactions) with temperature.

As expected, there were no significant changes in solution turbidity observed at 22 °C, suggesting that the monomeric ELP diblocks at this temperature did not form a network with fibrinogen (**Figure 6C**). At 32 °C, there was a significant increase in mixture turbidity in the presence of 10 μM GPRP-A80-I60 and GPRP-P40-I60 (Figure 6C, middle), suggesting that micelle formation at this temperature, coupled with engagement of fibrinogen holes by the displayed GPRP, led to network formation. At 42 °C, solutions of GPRP-A80-I60 and GPSP-A80-I60 were already above their cloud point, invalidating any data obtained from these wells (indicated by asterisks on the graph). On the other hand, solutions of GPRP-P40-I60 and GPSP-P40-I60 were below their cloud point, allowing us to evaluate the GPRP:fibrinogen (and control GPSP:fibrinogen) binding specificity at these temperaures. Turbidities of GPSP-P40-I60 with fibrinogen did not change significantly, indicating the absence of non-specific interactions at these elevated temperatures. Turbidities of GPRP-P40-I60 with fibrinogen were comparable to those at 32 °C, suggesting no significant disengagement of fibrinogen from these micelles at elevated temperatures.

Similar results were obtained in the presence of GPRP-A80-I60 and GPRP-P40-I60 mixed micelles, wherein no significant changes in mixture turbidity was observed at 22 °C, while an increase in turbidity was observed at 32 °C due to the micelle formation (Figure 6C, right). However, GPRP-A80-I60 mixed micelles with fibrinogen exhibit reduced mixture turbidities at elevated temperatures (42 °C), which suggests reduced interaction with fibrinogen at these temperatures. These results are congruent with our initial conceptual design where retraction of GPRP at elevated temperatures ($T > T_{t,A}$) should result in a non-fibrinogen-binding mixed micelle. Interestingly, we also observed a decrease in the turbidities of GPRP-P40-I60 mixed micelles with fibrinogen at elevated temperatures. Theoretically, there should not be changes in GPRP presentation for this mixed micelle since the P40-I60 section is common to both the functional GPRP-P40-I60 component and inactive GPSP-P40-I60 component.

2.9. Interaction of mixed micelles with fibrinogen fragment D using light scattering

For a more direct evaluation of the interaction between the GPRP-displaying mixed micelles and fibrinogen holes in real time, DLS was used to detect the changes in R_h as fibrinogen binds to the micelle. To avoid network formation and aggregation due to the multivalency of fibrinogen (a feature utilized in the previous set of experiments), fibrinogen fragment D comprising a single (instead of paired) set of holes was used. The binding strength of fibrin fragments displaying the GPRP peptide is known to be similar for fibrinogen and fibrinogen fragment D.[34] Interaction of fibrinogen fragment D with the micelles should result in an increase in R_h relative to the non-binding control, while disengagement of fibrinogen fragment D should result in a decrease in R_h.

A statistically significant change in R_h was observed for 10 μM GPRP-A80-I60, compared to the control GPSP-A80-I60, in the presence of 10 μM fragment D until particle aggregation (**Figure 7A**). A similar trend was observed for GPRP-P40-I60 against the control GPSP-P40-I60 although the R_h of both micelles exhibited a general decrease in response to temperature (**Figure 7B**). The moderate increase in R_h above ~43 °C may be associated with the denaturation of fibrinogen at these temperatures.

As the mixed micelles comprised four parts of GPSP-P40-I60 for each part of the functional component, it was unsurprising to observe the gradual decrease in R_h for all the mixed micelles in the presence of fragment D (Figure 7C, D). This may be suggestive of an unanticipated temperature-sensitive interaction of the outer P40 block with fibrinogen fragment D. Nonetheless, a significant difference in R_h was observed between the GPRP-A80-I60 and GPSP-A80-I60 mixed micelles, at 37 °C and below, but not at higher temperatures, a phenomenon we were anticipating in our initial conceptual design. Notably, the magnitude of the differences in R_h observed between the mixed micelles (GPRP-A80-I60 mix (+) versus GPSP-A80-I60 mix (+) in Figure 7C) was also smaller than that of the pure micelles (GPRP-A80-I60 (+) versus GPSP-A80-I60 (+) in Figure 7A). The surface of the GPRP-A80-I60 mixed micelle should comprise one part of the longer A80 block among four parts of the shorter P40 block. This may allow the bound fibrinogen fragment D to tuck into the corona of the mixed micelle, resulting in the smaller change in R_h. In contrast, the GPRP-A80-I60 pure micelle would comprise only the longer A80 blocks and we would expect any bound fibrinogen fragment D to cover the corona of the micelle, resulting in the larger change in R_h. Interestingly, no significant difference in R_h was observed for the GPRP-P40-I60 and GPSP-P40-I60 mixed micelles at all temperatures tested, even though an interaction between the GPRP-P40-I60 mixed micelles and fibrinogen was clearly observed for the turbidity assays within this temperature range.

3. Conclusion

Many stimuli-responsive systems reported in literature involve temperature- or pH-induced collapse or swelling of selective layers of two- or three-dimensional assemblies. In contrast, this work looks at the selective collapse of a polymer block within a particular layer of a three-dimensional assembly. The differential collapse of polymer blocks amongst non-collapsing polymer blocks poses unique challenges but is of significant value for the future development of multi-responsive 3-D assemblies that maintain structural integrity while displaying different ligands in response to environmental conditions. In this initial conceptual design, we designed a fibrinogen-binding micelle that disengages at elevated physiological temperatures as an intact micellar structure. Such a system has potential drug delivery applications as a circulating depot that will only be released *in situ* upon a specific trigger such as temperature (in our current design), pH or oxidative stress, for the delivery of cargo to the target site. The modular nature of such a self-assembling system also allows for the use of different peptide-displaying ELP diblocks within the same micellar assembly, creating micelles with multiple targeting motifs that can be used to tune their binding specificities. Given the extensive literature on ELPs and their transition characteristics, the use of ELPs is particularly advantageous to the design of such self-assembling, stimuli-responsive display systems. In addition, the ability to synthesize biopolymers with specific sequence compositions and functional handles facilitates the rapid characterization and study of the mixed assemblies formed using high throughput assays such as SYPRO Orange and ELISA. The defined compositions and molecular weights of the ELP diblocks used in this work also facilitated the formation of stable nanometer sized micelles with low polydispersities, allowing us to discern subtle changes in R_h due to the binding of fibrinogen fragment D to the peptide-displaying micelle.

One of the challenges faced in our development of this system was the selection of ELP diblock sequences that would continue to exhibit two distinct transition temperatures when fused together as a block copolymer. As shown in Ribeiro et al., the distinct transition temperatures of individual ELP blocks can be lost depending on their sequences, lengths, and arrangements in the final block copolymer.[35] Some of the previous iterations in our engineering of these ELP diblocks were unsuccessful for this reason (unpublished data). The stability of the micelles formed using this strategy is also dependent on the relative lengths of each block, giving rise to the type I "stable" and type II "growing" nanoparticles reported by Dreher et al.[12] an issue also encountered in some of our early iterations. Careful consideration must therefore be given to the choice of sequences used in the design of multi-responsive micellar assemblies involving more than the two species of ELP diblocks presented in this initial proof of concept.

The solid- and solution-phase affinity assays together with the DLS data suggest temperature-modulated avidities of the mixed micelles towards fibrinogen at different temperature regimes, likely due to the display of GPRP at lower temperatures, and retraction of GPRP at elevated temperatures, thus validating our starting hypothesis. However, it is noted that we did not achieve a clean switch in avidity from a fibrinogen-binding mixed micelle to a non-binding mixed micelle in all the assays presented. This may suggest interference of A80 block collapse by the neighboring P40 blocks in the mixed micelle.

Alternatively, the 1:4 molar ratio of GPRP-A80-I60-to-GPSP-P40-I60 used may not be optimized to dislodge fibrinogen from the collapsed GPRP-A80-I60 diblock. In particular, it is noted that fibrinogen fragment D was not released from GPRP-A80-I60-only micelles during the temperature ramp (Figure 7A), as expected from ELISA results suggesting that knob:hole interactions are not disrupted at elevated temperatures (Figure S3). The presence of an adequate proportion of GPSP-P40-I60 is therefore critical not only for maintaining

micelle structural integrity past $T_{t,A}$, but also for allowing successful disengagement of fibrinogen. Unfortunately, a 1:9 ratio of GPRP-A80-I60-to-GPSP-P40-I60, with proportionally fewer fibrinogen-binding GPRP moieties per micelle, resulted in fewer binding events per micelle, making it difficult to observe statistically significant differences between data sets. A different set of binding partners may thus be useful for evaluating the effect of mixed micelle composition on the efficiency of this system.

In conclusion, this work notes the successful creation of a simple self-assembling mixed micelle system that exhibits temperature-modulated avidities for the major blood circulating protein, fibrinogen. Such a system can potentially be used as a carrier for other proteins or drugs that will only be released *in situ* in response to stimuli intrinsic to the local milieu by using the appropriate ELP blocks. For example, Simnick et al. have recently reported the successful targeting of peptide-decorated self-assembled ELP micelles to tumors in mice.[36] Since the structural integrity of the micelle should be preserved at physiological temperatures by virtue of the P40-I60 ELP diblock, such a carrier system can theoretically be circulated continuously intravenously, acting as a reservoir that will only release its cargo locally when and where needed. The use of multiple species of ELP diblocks within the same micellar assembly would also facilitate the engineering of the release of different cargo in response to different stimuli.

4. Experimental Section

ELP design and production

ELPs of the desired transition temperatures were designed using the hydrophobicity scale proposed by Urry et al. as a general guide.[7] Sequences coding for the desired ELPs were custom ordered and amplified by recursive directional ligation.[37] These sequences were inserted into modified pET15 expression vectors, which were then transformed into BL21(DE3) for recombinant protein production. The expressed ELP diblocks were purified using inverse transition cycling.[10] Further details on the cloning process and protein verification can be found in the supplementary information. Briefly, the following ELP diblocks were created: GPRP-A80-I60, GPSP-A80-I60, GPRP-A80-I60-C, GPSP-A80-I60-C, GPRP-P40-I60, GPSP-P40-I60, GPRP-P40-I60-C, GPSP-P40-I60-C, where I60 is $[(VPGIG)_4VPGVG]_{60}$, A80 is $[(VPGAG)_4VPGVG]_{80}$, and P40 is $[(VPGPG)_4VPGVGGS]_{40}$. In addition, the indicated N-terminal GPRP is the fibrinogen-binding peptide sequence while GPSP is the corresponding non-binding peptide control, and the C-terminal cysteine confers a functional handle for conjugation to maleimide-activated surfaces or fluorescent labels. The peptide sequences of the ELPs produced are summarized in **Table 2**.

Note: Instances of "GPRP-A80-I60 mix" and "GPSP-A80-I60 mix" used in this paper refer to 1:4 mixtures of one part of GPRP-A80-I60 or GPSP-A80-I60, with four parts of GPSP-P40-I60 respectively. In other words, 2 μм of GP(R/S)P-A80-I60 and 8 μм of GPSP-P40-I60 for a 10 μм ELP solution. Similarly, instances of "GPRP-P40-I60 mix" and "GPSP-P40-I60 mix" used in this paper refer to 1:4 mixtures of one part of GPRP-P40-I60 or GPSP-P40-I60, with four parts of GPSP-P40-I60 respectively.

ELP transition characterization

Temperature-dependent transitions of the ELP diblocks were monitored using a protein-binding fluorescent dye, SYPRO Orange (Invitrogen #S6650). Following a methodology analogous to that reported by Niesen et al.,[38] 5× SYPRO Orange (final concentration) was added to 96-well optical PCR plates containing varying concentrations of the ELP in TBS +Ca (25 mм Tris-HCl pH 7.4, 137 mм NaCl, 5 mм CaCl$_2$). The PCR plate was sealed with

optical adhesive film and placed into the ABI StepOnePlus real-time PCR system (Life Technologies, Carlsbad, CA). Samples were heated at 0.9 °C min^{-1} from 10 °C to 65 °C and the raw data from the ROX (6-carboxyl-X-rhodamine) channel were used for analysis.

Cloud point measurements

The cloud point of 10 μ$_M$ protein solutions was sampled using the cloud point protocol built into the FP900 thermo system for the FP81HT MBC temperature chamber (Mettler-Toledo, Columbus, OH). Solutions were loaded into the recommended melting point capillaries and inserted into the chamber pre-equilibrated at 25 °C. A 1 °C min^{-1} ramp was used and the solution cloud points were evaluated using the default criteria (i.e. a 4% transmittance drop of the initial value).

Micelle characterization via light scattering

Particles containing the ELP diblocks were analyzed using dynamic light scattering (DLS). Briefly, solutions of the ELP diblock were prepared on ice and transferred to a black clear-bottom 384-well plate. The plate was spun down at 3000 × g for 10 min at 4 °C to eliminate air bubbles before placing in the DynaPro plate reader (Wyatt, Santa Barbara, CA). Following a 15-min thermal equilibration step at 25 °C, 20 reads of 20 s acquisitions were recorded for each well. This process was repeated at increments of 1 °C or 2 °C (where indicated) until particle aggregation led to a heterogenous distribution of micron-sized particles generating poor correlation data. Data were collected for at least 4 independently prepared runs. For statistical analysis, data from 9 runs were used. Where indicated, 10 μ$_M$ of fibrinogen fragment D was added to wells containing 10 μ$_M$ ELP diblocks. The purification of fragment D from a plasmin digest of fibrinogen has been described in a previous publication.[39]

The weight average molar mass (Mw) and root mean square radii (R_{rms}) of assembled ELP particles was measured via multiangle light scattering (MALS) using a DAWN-EOS detector (Wyatt Technology Corporation, Santa Barbara, CA) equipped with a temperature-regulated K5 flow cell with a GaAs laser light source (λ = 685 nm). The principles employed in MALS measurements has been described previously.[40] In brief, suspensions of polymers scatter light with an intensity governed by the molar mass of the polymer and the concentration. Angular dependence to the scattering is observed for assembled nanostructures, where extrapolation to 0° scattering angle allows accurate measurements of particle molar mass and R_{rms}, according to the following equation at low polymer concentration,

$$\frac{R_\theta}{Kc} = Mw \left[1 - \left(\frac{16\pi^2}{3\lambda^2} \right) \langle r_{rms} \rangle^2 \sin^2 \left(\frac{\theta}{2} \right) \right] \quad (1)$$

where $K = 4\pi^2 n_0^2 \lambda^{-4} N_A^{-1} (dn/dc)^2$, c is the polymer concentration, $R(\theta)$ is the Rayleigh ratio, and λ is the wavelength of light. For the ELP particles investigated in this work, extrapolations were performed using the Debye method for constructing the Debye plot.[40] Using Equation 1, the Mw and R_{rms} is derived from the intercept and slope of the best fit to the Debye plot. Data collection and subsequent light scattering analysis was performed using the Astra software Version 5.3.4.14 (Wyatt Technology Corporation, Santa Barbara, CA). For accurate measurements of particle molar mass, the ELP concentration was measured using an online Optilab rEX differential refractometer (Wyatt Technology Corporation), assuming a dn/dc value of 0.185.[41] All ELP peptides were diluted in TBS+Ca to a concentration of 3 μ$_M$ and administered to the MALS using a Calypso controlled mixing device (Wyatt Technology Corporation), equipped with in-line Anodisc 0.1 μm filters

(Whatman, Kent, UK). The Mw and R_{rms} of particles were measured in several replicates ($n = 4$) at 35 °C after thermal equilibration (30 min) within the MALS.

Atomic Force Microscopy (AFM)

Samples were analyzed under ambient conditions at 22 °C using the Asylum Research MFP-3D AFM (Santa Barbara, CA). Imaging was performed and processed using the MFP-3D software written in the IgorPro environment (WaveMetrics Inc., Lake Oswego, OR). Non-contact mode silicon cantilevers with an aluminum reflex coating, purchased from Nanoworld, were used (force constant = 42 N m^{-1}, resonant frequency = 320 kHz). Solutions at an ELP concentration of 5.0 μM were prepared in TBC+Ca. Samples were prepared by passive adsorption by incubating glass coverslips in the protein solution at 37 °C for 10 min followed by dipping in deionized water to rinse. Samples were then gently dried under nitrogen. The average particle heights of GPRP-A80-I60, GPSP-P40-I60 and the mixture (1:4) were calculated from 10 particles in a total of 3 images for each solution. The particle height was determined by drawn line profiles using the analysis panel in the MFP-3D software.

Mixed micelle formation via FRET

ELP diblocks with C-terminal cysteines were labeled with either the Alexa Fluor 488 or Alexa Fluor 546 (Invitrogen) via sulfhydryl-maleimide chemistry following the manufacturer's recommended protocol. Combinations of AF488-labeled, AF546-labeled and unlabeled ELP diblocks were added to black clear-bottom 384-well plates for a total concentration of 1 μM ELP diblock per well (higher concentrations of labeled protein saturated the fluorescence detectors). The 384-well plate was sealed with optical adhesive film and incubated in the H4 Synergy microplate reader (Biotek, Winooski, VT) at 25 °C for 15 min before excitation at 470 nm and acquiring the emission spectrum from 500 to 700 nm using a 2 nm step size. The emission spectra were monitored at successive 5 °C intervals (30, 35, 40, 45, 50, 55, 60 °C) with a 15-min incubation time allowed for thermal equilibration with each stepwise increase. Changes in the emission peaks were normalized against respective control wells containing only AF488-labeled or AF546-labeled protein (for evaluating $I^0_{Em,a}$ and $I^0_{Em,d}$) and designated as fold change in emission ($F_a = I_{Em,a}/I^0_{Em,a}$ and $F_d = I_{Em,d}/I^0_{Em,d}$).

For pre-formed micelles, 1 μM of the ELP diblocks were prepared in the wells of a 384-well plate, which was then incubated at 35 °C for 1 h. Equal volumes of the indicated ELP diblocks were then mixed together using a multi-channel pipette with pre-warmed pipette tips. The emission spectra of these mixtures were taken at 35 °C (pre-cooling data). The plate was then allowed to cool to room temperature for 1 h. The emission spectra of these cooled mixtures were taken at 25 °C. The readings from these spectra were used for evaluating $I^0_{Em,a}$ and $I^0_{Em,d}$ used in the calculations. Then, the plate was incubated at 35 °C for 15 min before taking the emission spectra at 35 °C (post-cooling data). For the premixed controls, the indicated ELP diblocks were mixed together prior to the initial 1-h 35 °C incubation and read at 35 °C.

Solid-phase fibrinogen binding assays

An enzyme-linked immunosorbent assay (ELISA) was used to establish the affinity of fibrinogen for ELP diblocks covalently immobilized on maleimide-activated plates via their C-terminal cysteines as described previously.[39] Due to the sensitivity of ELP transition characteristics to the Hofmeister effect,[41] all assays were conducted in a Tris-based buffer (TBS+Ca) in place of the phosphate buffer recommended in the manufacturer's protocol. Briefly, varying concentrations of sulfhydryl-containing protein/peptides were conjugated to pre-blocked maleimide-activated plates (Pierce, Thermo Scientific, Rockford, IL), which

were then quenched with cysteine. ELP-coated wells were incubated with fibrinogen (#FIB3, Enzyme Research Laboratories, South Bend, IN) and the remaining bound fibrinogen after washing was detected using HRP-conjugated goat anti-fibrinogen antibody (MP Biomedicals #55239) and 1-Step Ultra TMB-ELISA (Pierce) with 1 $_M$ H_2SO_4 as the stop solution. All intervening wash steps were conducted in TBS+Ca + 0.5% Tween-20. Results were normalized to GPSPFPAC-coated wells (0%) and GPRPFPAC-coated wells (100%).

Solid-phase mixed micelle binding assays

A plate-based assay conceptually similar to an ELISA was used to establish the affinity of ELP mixed micelles for immobilized fibrinogen on black 96-well plates. Briefly, fibrinogen was passively adsorbed on 96-well plates at 0.1 mg mL^{-1} for 3 h at room temperature. The plates were washed, then blocked with 1% BSA for 1 h at room temperature. The wells were washed with pre-warmed buffer before adding preequilibrated mixed ELP micelles comprising 2 $_{\mu M}$ unlabeled ELP (the "functional component") and 8 $_{\mu M}$ labeled GPSP-P40-I60-AF546 (non-fibrinogen binding). The plates were incubated at the desired temperatures for 1 h, washed with pre-warmed TBS+Ca to remove the unbound protein, then allowed to equilibrate to room temperature before fluorescence measurements (λ_{Ex} = 540 nm, λ_{Em} = 573 nm) were taken. Background fluorescence, evaluated from control BSA-coated wells, was subtracted from the data, with the result reported as relative fluorescence units (RFU).

Solution-phase turbidity assays

A plate-based assay was used to establish the affinity of ELP micelles for fibrinogen in solution in clear 384-well plates. ELP mixtures and fibrinogen were equilibrated to the desired temperatures before addition to the wells. The plate was incubated at the desired temperature for 1 h before turbidity measurements (λ = 350 nm) were taken in the pre-heated plate reader. Background absorbance, evaluated from control wells without fibrinogen was subtracted from the data, with the result reported as relative turbidity.

Statistical analysis

All data was acquired from at least 3 sets of triplicate experiments, and presented as mean ± SD unless otherwise stated. Two-tailed t-tests were used to evaluate statistical significance ($p < 0.05$) where indicated.

Supplementary Material

Refer to Web version on PubMed Central for supplementary material.

Acknowledgments

Glossary of Protein Nomenclature

I60	ELP block with the lowest transition temperature; $T_{t,I}$ near room temperature
A80	ELP block with the middle transition temperature; $T_{t,A}$ slightly above physiological temperature
P40	ELP block with the highest transition temperature (if any); $T_{t,P}$ above temperature window examined in the paper

GPRP	peptide sequence that binds to fibrinogen
GPSP	peptide sequence that does not bind to fibrinogen
GPRP-A80-I60	fibrinogen-binding collapsible ELP diblock
GPSP-A80-I60	non-binding collapsible ELP diblock
GPRP-P40-I60	fibrinogen-binding non-collapsible ELP diblock
GPSP-P40-I60	non-binding collapsible ELP diblock

References

1. Hoffman AS, Stayton PS. Progress in Polymer Science. 2007; 32:922.

2. Cole MA, Voelcker NH, Thissen H, Griesser HJ. Biomaterials. 2009; 30:1827. [PubMed: 19144401]

3. Ganta S, Devalapally H, Shahiwala A, Amiji M. J Control Release. 2008; 126:187. [PubMed: 18261822]

4. Chow D, Nunalee ML, Lim DW, Simnick AJ, Chilkoti A. Mater Sci Eng R Rep. 2008; 62:125. [PubMed: 19122836]

5. Rabotyagova OS, Cebe P, Kaplan DL. Biomacromolecules. 2011; 12:269. [PubMed: 21235251]

6. Urry DW, Trapane TL, Prasad KU. Biopolymers. 1985; 24:2345. [PubMed: 4092092]

7. Urry DW, Gowda DC, Parker TM, Luan CH, Reid MC, Harris CM, Pattanaik A, Harris RD, R. D. Biopolymers. 1992; 32:1243. [PubMed: 1420991]

8. Reguera J, Lagarón JM, Alonso M, Reboto V, Calvo B, Rodriguez Cabello JC. Macromolecules. 2003; 36:8470.

9. McPherson DT, Xu J, Urry DW. Protein Expr Purif. 1996; 7:51. [PubMed: 9172783]

10. Meyer DE, Chilkoti A. Nat Biotechnol. 1999; 17:1112. [PubMed: 10545920]

11. Trabbic-Carlson K, Liu L, Kim B, Chilkoti A. Protein Sci. 2004; 13:3274. [PubMed: 15557268]

12. Dreher MR, Simnick AJ, Fischer K, Smith RJ, Patel A, Schmidt M, Chilkoti A. J Am Chem Soc. 2008; 130:687. [PubMed: 18085778]

13. Lee TAT, Cooper A, Apkarian RP, Conticello VP. Adv. Mater. 2000; 12:1105.

14. Fujita Y, Mie M, Kobatake E. Biomaterials. 2009; 30:3450. [PubMed: 19324406]

15. Nagapudi K, Brinkman WT, Leisen J, Thomas BS, Wright E, Haller C, Wu X, Apkarian RP, Conticello VP, Chaikof EL. Macromolecules. 2005; 38:345.

16. Sallach RE, Cui W, Wen J, Martinez A, Conticello VP, Chaikof EL. Biomaterials. 2009; 30:409. [PubMed: 18954902]

17. Rodriguez-Cabello JC, Martin L, Girotti A, Garcia-Arevalo C, Arias FJ, Alonso M. Nanomedicine. 2011; 6:111. [PubMed: 21182423]

18. Urry DW, Haynes B, Zhang H, Harris RD, Prasad KU. Proc Natl Acad Sci U S A. 1988; 85:3407. [PubMed: 2897120]

19. Urry DW, Urry KD, Szaflarski W, Nowicki M. Adv Drug Deliv Rev. 2010; 62:1404. [PubMed: 20655344]

20. Li B, Alonso DO, Daggett V. J Mol Biol. 2001; 305:581. [PubMed: 11152614]

21. Yamaoka T, Tamura T, Seto Y, Tada T, Kunugi S, Tirrell DA. Biomacromolecules. 2003; 4:1680. [PubMed: 14606895]

22. Krukau A, Brovchenko I, Geiger A. Biomacromolecules. 2007; 8:2196. [PubMed: 17567170]

23. Reiersen H, Rees AR. Biochemistry. 1999; 38:14897. [PubMed: 10555972]

24. Megeed Z, Winters RM, Yarmush ML. Biomacromolecules. 2006; 7:999. [PubMed: 16602713]

25. Stabenfeldt SE, Gossett JJ, Barker TH. Blood. 2011; 116:1352. [PubMed: 20484082]

26. Litvinov RI, Gorkun OV, Owen SF, Shuman H, Weisel JW. Blood. 2005; 106:2944. [PubMed: 15998829]

27. Laudano AP, Doolittle RF. Proc Natl Acad Sci U S A. 1978; 75:3085. [PubMed: 277910]

28. Urry DW. J Phys Chem B. 1997; 101:11007.

29. Meyer DE, Chilkoti A. Biomacromolecules. 2004; 5:846. [PubMed: 15132671]

30. Trabbic-Carlson K, Meyer DE, Liu L, Piervincenzi R, Nath N, LaBean T, Chilkoti A. Protein Eng Des Sel. 2004; 17:57. [PubMed: 14985538]

31. Senisterra GA, Jr PJ. Finerty, Mol Biosyst. 2009; 5:217.

32. Weisel JW, Nagaswami C. Biophys J. 1992; 63:111. [PubMed: 1420861]

33. Soon AS, Lee CS, Barker TH. Biomaterials. 2011; 32:4406. [PubMed: 21435714]

34. Litvinov RI, Gorkun OV, Owen SF, Shuman H, Weisel JW. Blood. 2005; 106:2944. [PubMed: 15998829]

35. Ribeiro A, Arias FJ, Reguera J, Alonso M, Rodriguez-Cabello JC. Biophys J. 2009; 97:312. [PubMed: 19580769]

36. Simnick AJ, Amiram M, Liu W, Hanna G, Dewhirst MW, Kontos CD, Chilkoti A. J Control Release. 2011; 155:144. [PubMed: 21763734]

37. Meyer DE, Chilkoti A. Biomacromolecules. 2002; 3:357. [PubMed: 11888323]

38. Niesen FH, Berglund H, Vedadi M. Nat Protoc. 2007; 2:2212. [PubMed: 17853878]

39. Soon AS, Stabenfeldt SE, Brown WE, Barker TH. Biomaterials. 2010; 31:1944. [PubMed: 19914710]

40. Andersson M, Wittgren B, Wahlund KG. Anal Chem. 2003; 75:4279. [PubMed: 14632147]

41. Wen J, Arakawa T. Anal Biochem. 2000; 280:327. [PubMed: 10790320]

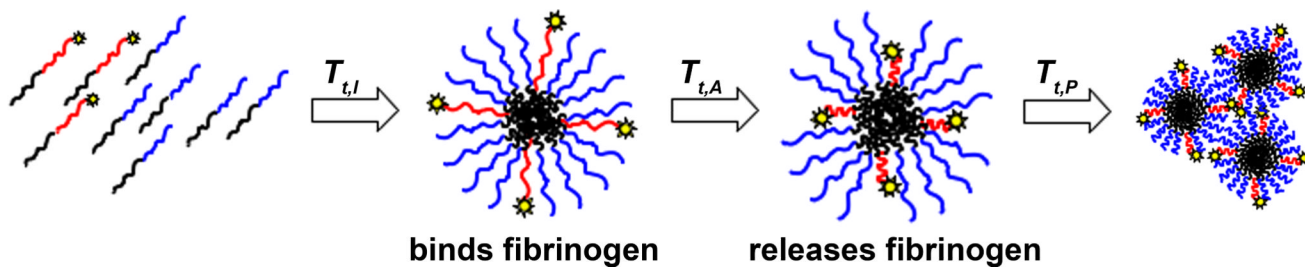**binds fibrinogen** **releases fibrinogen**

Figure 1.
Schematic depicting the idealized assembly and collapse of the engineered ELP diblocks in response to increasing temperature (left to right). ELPs are protein chains known to transition from an extended soluble structure to a collapsed insoluble structure above their transition temperature, T_t. The I60 ELP block is depicted in black, A80 in red, and P40 in blue, where $T_{t,I} < T_{t,A} < T_{t,P}$. Below $T_{t,I}$, both A80-I60 and P40-I60 exist as free protein chains. Above $T_{t,I}$, the hydrophobic collapse of I60 results in the self-assembly of mixed micelles that display fibrinogen-binding peptides (depicted as yellow stars). Above $T_{t,A}$, the collapse of A80 results in the retraction of fibrinogen-binding peptides and concomitant release of fibrinogen. Above $T_{t,P}$, the collapse of P40 results in aggregation of the proteins, forming micron-sized aggregates.
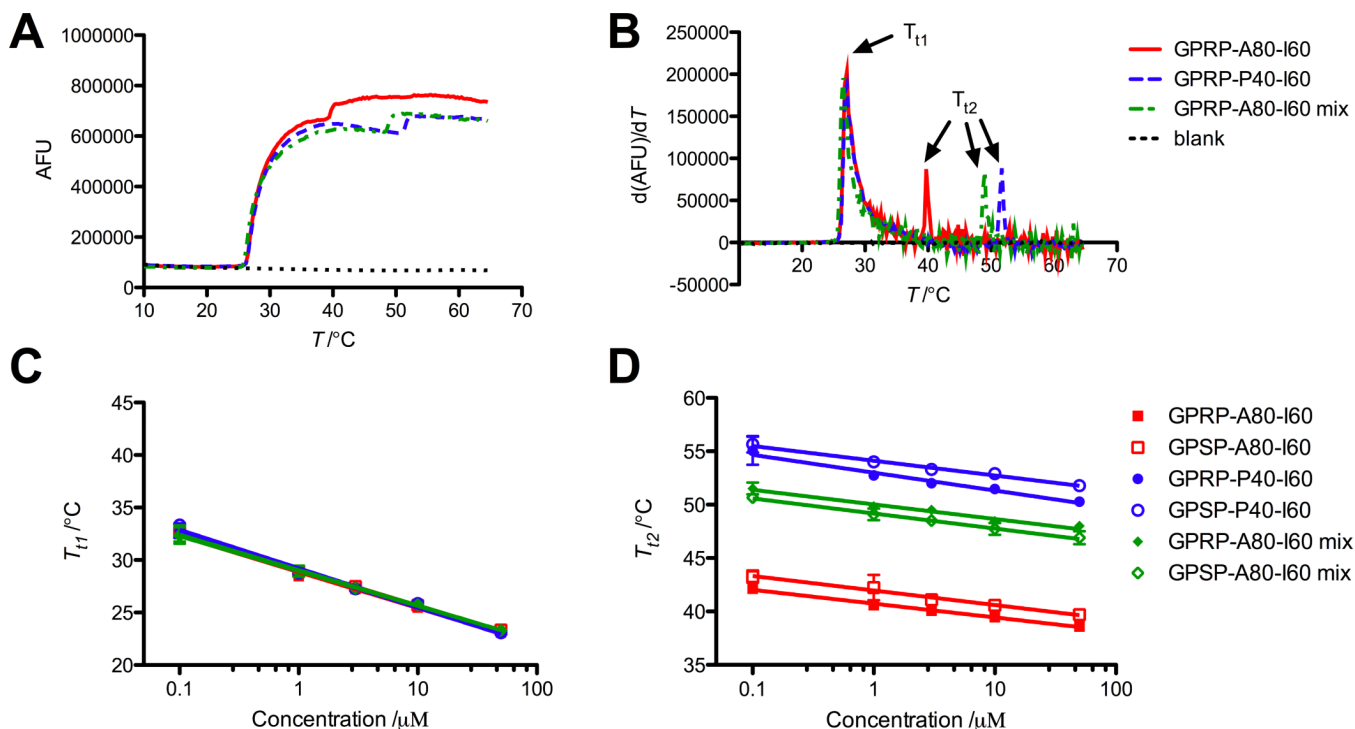
Figure 2.
Temperature transition characteristics evaluated using SYPRO Orange. (A) Representative fluorescence readouts from 10 μ_M solutions of GPRP-A80-I60, GPSP-P40-I60 and a 1:4 mixture of GPRP-A80-I60-to-GPSP-P40-I60 upon a 0.9 °C min^{-1} temperature ramp. (B) The calculated derivatives of the fluorescence curves used to obtain the transition temperatures of the solutions. Two distinct transition temperatures (T_{t1}, T_{t2}) were observed for all solutions within the concentration range tested. (C) Plot of T_{t1} as a function of total ELP concentration showing a good overlap of the data points from the different solutions tested. (D) Plot of T_{t2} as a function of total ELP concentration showing dependence of this transition on mixture composition. Data reported as mean ± SD with a semi-log fit as described in Meyer and Chilkoti.[29]
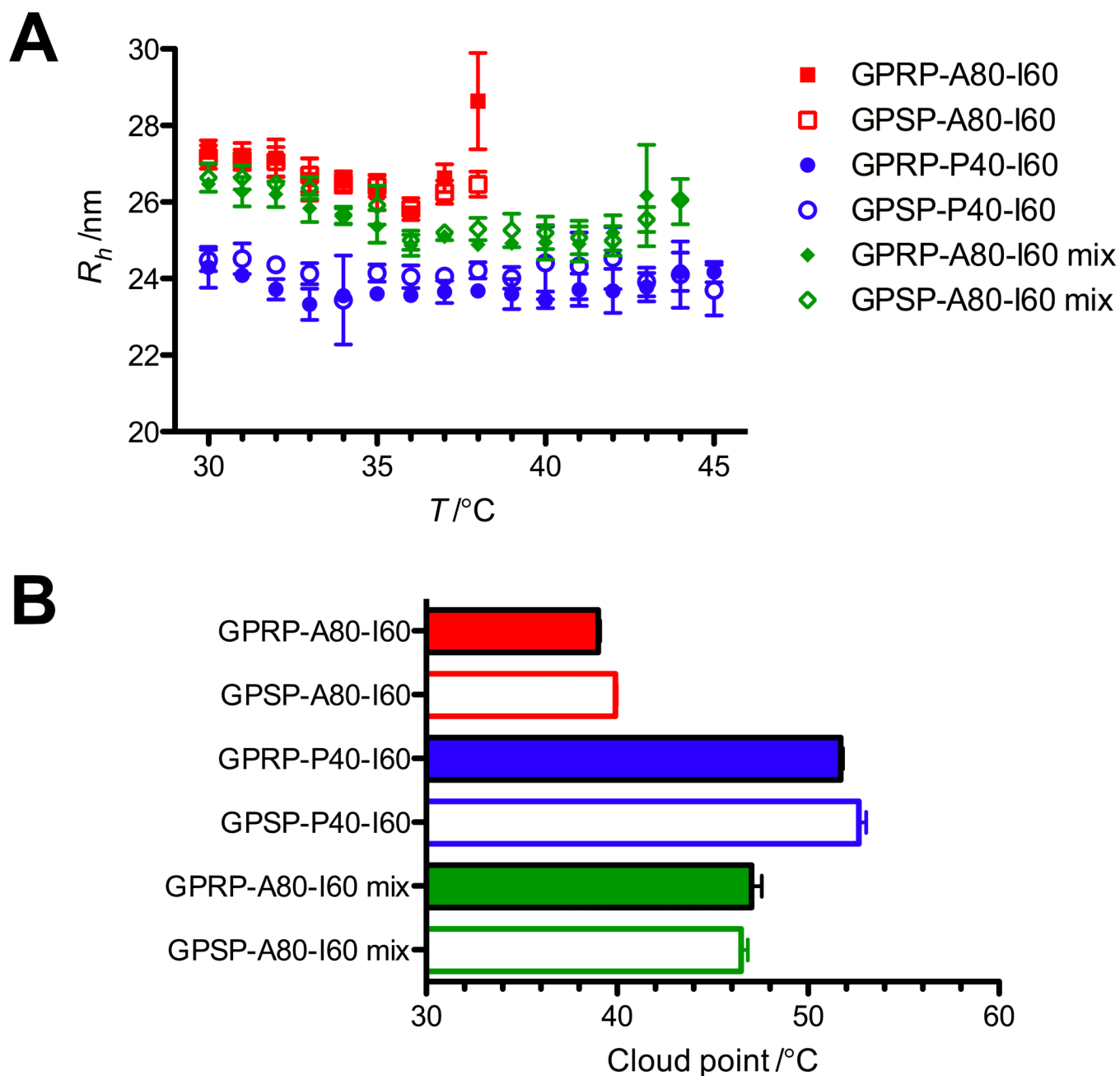
Figure 3.
DLS data of micelles. (A) Hydrodynamic radius (R_h) of 10 μM protein solutions calculated using the regularization fit provided by the DYNAMICS® software. Data reported as mean ± SD using averaged data (from 20 acquisitions) from 4 independent runs. (B) Cloud point of 10 μM protein solutions acquired from the Mettler Toledo cloud point measuring cell. Mean ± SD ($n = 9$).
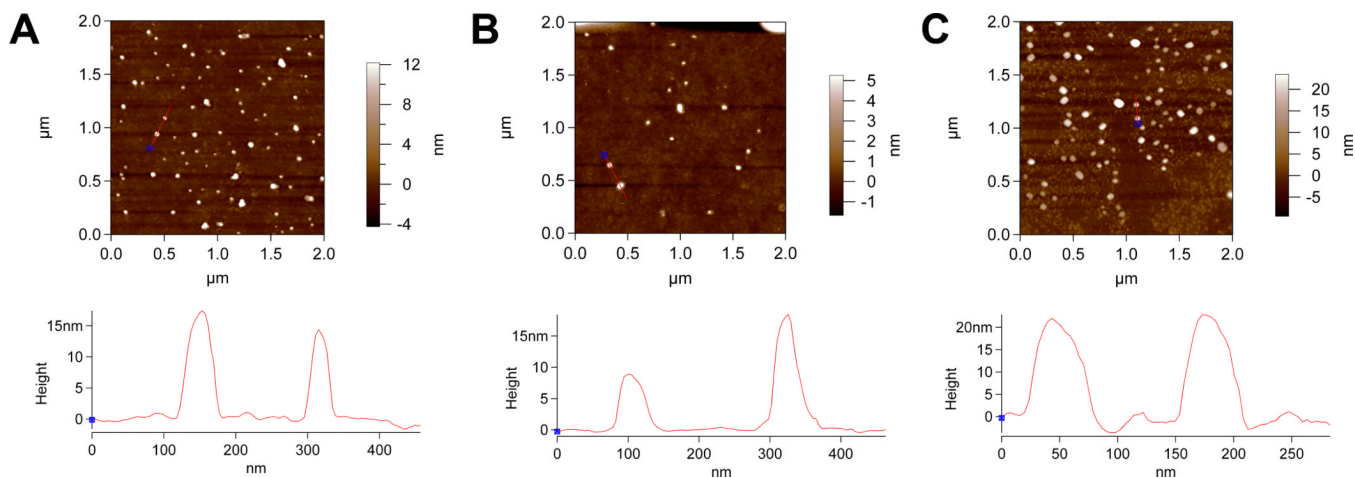
Figure 4.
AFM imaging of micelles. Representative height traces of GPRP-A80-I60 micelles (A), GPSP-P40-I60 micelles (B) and 1:4 mixed micelles (C) demonstrating the use of a line profile and section graph for calculating average particle height. Scan size = 2.00 μm, scan rate = 0.80 Hz, scan points = 512, scan lines = 512.
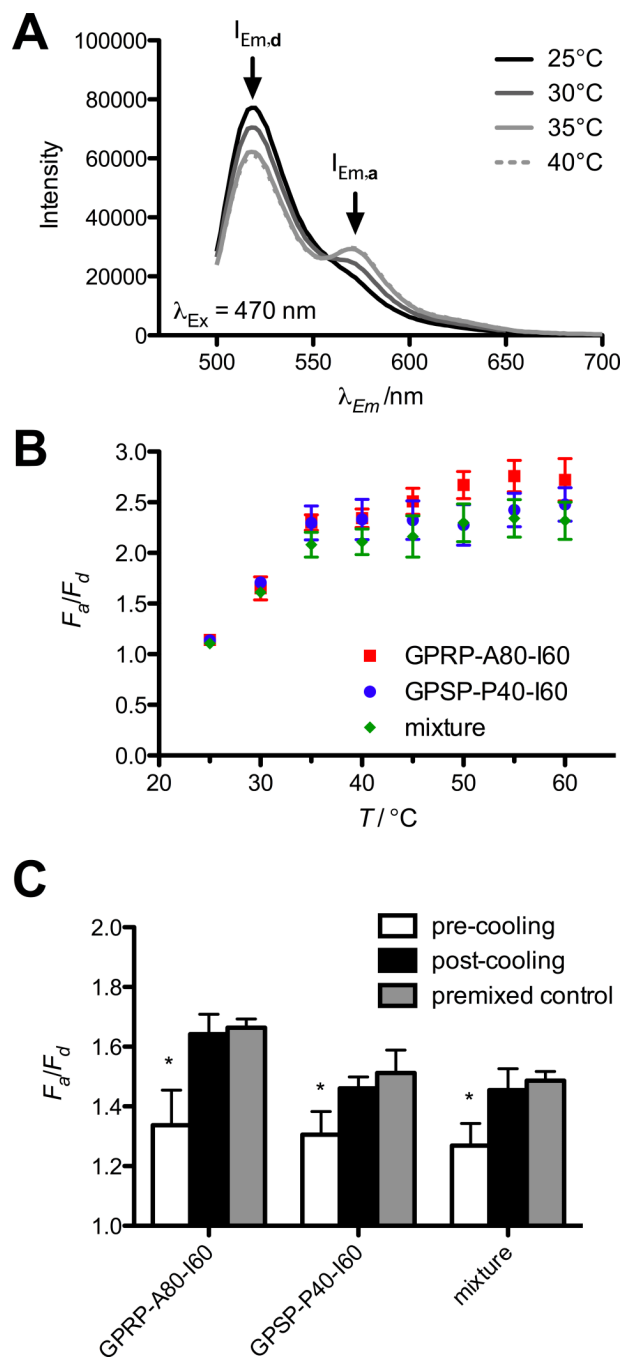
Figure 5.
Formation of mixed micelles demonstrated using FRET. (A) Representative emission spectrum obtained from an equimolar mixture of GPRP-A80-I60-AF488 and GPSP-P40-I60-AF546 (1 μM final protein concentration) excited at 470 nm at various temperatures. Emission peaks of donor AF488 ($I_{Em,d}$) and acceptor AF546 ($I_{Em,a}$) are indicated by arrows. (B) Results are reported as fold change in $I_{Em,a}$ ($F_a = I_{Em,a}/I^0_{Em,a}$) divided by fold change in $I_{Em,d}$ ($F_d = I_{Em,d}/I^0_{Em,d}$) for equimolar mixtures of GPRP-A80-I60-AF488 and GPRP-A80-I60-AF546 (squares), GPSP-P40-I60-AF488 and GPSP-P40-I60-AF546 (circles), GPRP-A80-I60-AF488 and GPSP-P40-I60-AF546 (diamonds) as a function of temperature. (C) F_a/

F_d for mixtures of pre-formed micelles of GPRP-A80-I60-AF488 and GPRP-A80-I60-AF546 (GPRP-A80-I60), GPSP-P40-I60-AF488 and GPSP-P40-I60-AF546 (GPSP-P40-I60), GPRP A80-I60-AF488 and GPSP-P40-I60-AF546 (mixture) at 35 °C, before and after a 1-h incubation at room temperature.
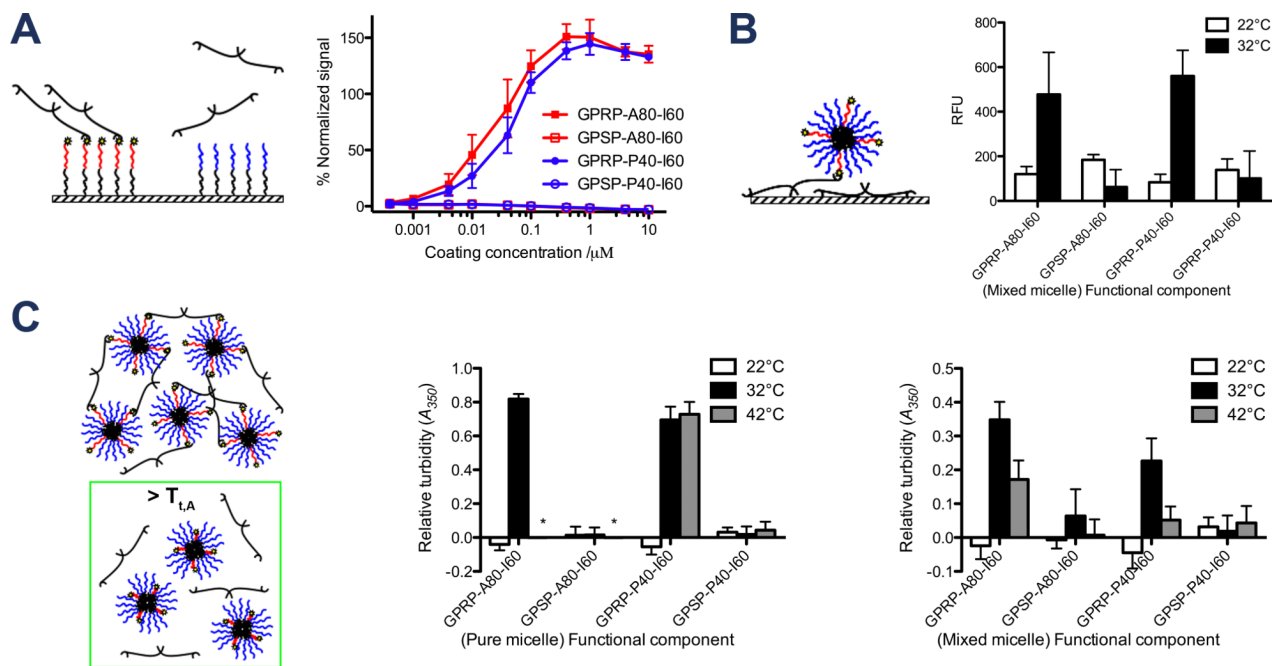
Figure 6.
Characterization of ELP affinity for fibrinogen as a function of temperature. (A) Specific binding of fibrinogen to immobilized GPRP-A80-I60 via the fibrinogen-binding peptide in an ELISA setup. ELISA plate readouts (λ = 450 nm) were normalized to GPRPFPAC-coated control wells and reported as % normalized signal as a function of coating concentration. (B) Temperature-responsive binding of fluorescently-labeled mixed micelles to immobilized fibrinogen in 96-well plate setup. Fluorescence readouts reflecting the amount of GPSP-P40-I60-AF546 recruited to the immobilized fibrinogen by the indicated unlabeled "functional component" at 22°C and 32°C are reported as relative fluorescent units (λ_{Ex} = 540 nm, λ_{Em} = 573 nm). (C) Temperature-responsive binding between micelles and fibrinogen in solution at 22°C, 32°C, 42°C. Absorbance readouts reflecting the interaction of the pure micelles (comprising the indicated ELP diblocks only) or mixed micelles (1:4 mixtures of the indicated functional component with GPSP-P40-I60) with fibrinogen are reported as relative turbidity (λ = 350 nm). Asterisks indicate wells in which the ELP-only controls precipitated out.
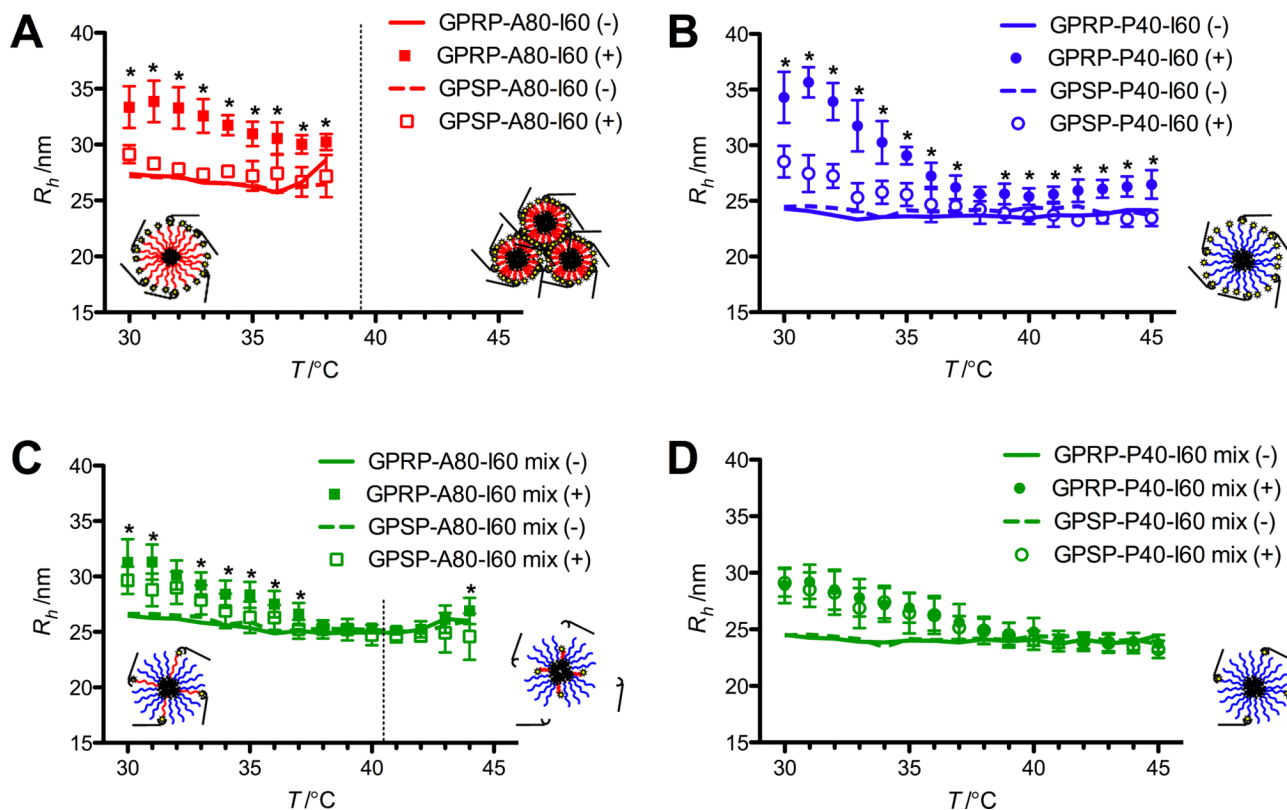
Figure 7.
Characterization of interaction of mixed micelles with fibrinogen fragment D in response to a temperature ramp via DLS. R_h is reported for pure micelles (A, B) and mixed micelles (C, D) in the presence (closed and open symbols) and absence (solid and dashed lines) of fibrinogen fragment D. Standard deviations for data points in the absence of fragment D are not shown for visual clarity. T_{t2} for the respective GPRP-A80-I60 compositions (10 μM for the pure micelle and 2 μM for the mixed micelle) based on the SYPRO Orange assay (see Figure 2) is shown as dotted lines. The hypothesized micelle configuration in the presence of fibrinogen fragment D below (left of the dotted line) and above (right of the dotted line) this transition temperature is shown as cartoons on the respective graphs. T_{t2} for GPRP-P40-I60 (> 50 °C) was not attained in this assay. Asterisks indicate statistically significant differences between data sets in the presence of fragment D at each temperature as evaluated using the unpaired Student's t-test.

Table 1

Summary of micelle properties measured via MALS and DLS at 35 °C, reported as mean ± SD (n = 4).

ELP	R_{rms} [nm]	R_h [nm]	ρ	Mw_{ELP} [10³ Da]	Mw [10⁶ Da]	Z
GPRP-A80-I60	17.0 ± 1.0	26.2 ± 0.5	0.63	57.5	11 ± 2	190
GPSP-P40-I60	15.2 ± 0.3	23.6 ± 0.2	0.64	43.9	8.4 ± 0.4	190
mixture (1:4)	15.3 ± 0.2	25.4 ±0.4	0.60	46.7	9.3 ± 0.2	199

[a)] Average molecular weight of the given ELP based on its amino acid sequence. In the case of the mixture (1 part GPRP-A80-I60 with 4 parts GPSP-P40-I60), Mw_{elp} was calculated using a weighted average.

Table 2

Peptide sequence of the ELPs used in this publication.

ELP	Peptide sequence (in standard amino acid single-letter abbreviations)
GPRP-A80-I60	GPRPFPAAGPG[VGVPGAGVPGAGVPGAGVPGAGVPG]$_{16}$ [VGVPGIGVPGIGVPGIGVPGIGVPG]$_{12}$ WP
GPSP-A80-I60	GPSPFPAAGPG[VGVPGAGVPGAGVPGAGVPGAGVPG]$_{16}$ [VGVPGIGVPGIGVPGIGVPGIGVPG]$_{12}$ WP
GPRP-P40-I60	GPRPFPAAGPG[VGGSVPGPGVPGPGVPGPGVPGPGVPG]$_{8}$ [VGVPGIGVPGIGVPGIGVPGIGVPG]$_{12}$ WP
GPSP-P40-I60	GPSPFPAAGPG[VGGSVPGPGVPGPGVPGPGVPGPGVPG]$_{8}$ [VGVPGIGVPGIGVPGIGVPGIGVPG]$_{12}$ WP
GPRP-A80-I60-C	GPRPFPAAGPG[VGVPGAGVPGAGVPGAGVPGAGVPG]$_{16}$ [VGVPGIGVPGIGVPGIGVPGIGVPG]$_{12}$ WPGGC
GPSP-A80-I60-C	GPSPFPAAGPG[VGVPGAGVPGAGVPGAGVPGAGVPG]$_{16}$ [VGVPGIGVPGIGVPGIGVPGIGVPG]$_{12}$ WPGGC
GPRP-P40-I60-C	GPRPFPAAGPG[VGGSVPGPGVPGPGVPGPGVPGPGVPG]$_{8}$ [VGVPGIGVPGIGVPGIGVPGIGVPG]$_{12}$ WPGGC
GPSP-P40-I60-C	GPSPFPAAGPG[VGGSVPGPGVPGPGVPGPGVPGPGVPG]$_{8}$ [VGVPGIGVPGIGVPGIGVPGIGVPG]$_{12}$ WPGGC